Metadata of the chapter that will be visualized online

Chapter Title	Formation and Nanoscale Characterization of Asymmetric Supported Lipid Bilayers Containing Raft-Like Domains	
Copyright Year	2022	
Copyright Holder	The Author(s), under exclusive license to Springer Science+Business Media, LLC, part of Springer Nature	
Corresponding Author	Family Name	**Vázquez**
	Particle	
	Given Name	**Romina F.**
	Suffix	
	Division	Instituto de Investigaciones Bioquímicas de La Plata (INIBIOLP), CCT-La Plata, CONICET, Facultad de Ciencias Médicas
	Organization	Universidad Nacional de La Plata
	Address	La Plata, Argentina
	Division	Departamento de Química, Facultad de Ciencias Exactas
	Organization	Universidad Nacional de La Plata
	Address	La Plata, Argentina
	Email	rvazquez@quimica.unlp.edu.ar
Author	Family Name	**Ovalle-García**
	Particle	
	Given Name	**Erasmo**
	Suffix	
	Division	Instituto de Ciencias Físicas
	Organization	Universidad Nacional Autónoma de México
	Address	Cuernavaca, México
Author	Family Name	**Antillón**
	Particle	
	Given Name	**Armando**
	Suffix	
	Division	Instituto de Ciencias Físicas
	Organization	Universidad Nacional Autónoma de México
	Address	Cuernavaca, México
Author	Family Name	**Ortega-Blake**
	Particle	
	Given Name	**Iván**
	Suffix	
	Division	Instituto de Ciencias Físicas

	Organization	Universidad Nacional Autónoma de México
	Address	Cuernavaca, México
Author	Family Name	**Muñoz-Garay**
	Particle	
	Given Name	**Carlos**
	Suffix	
	Division	Instituto de Ciencias Físicas
	Organization	Universidad Nacional Autónoma de México
	Address	Cuernavaca, México
Corresponding Author	Family Name	**Maté**
	Particle	
	Given Name	**Sabina M.**
	Suffix	
	Division	Instituto de Investigaciones Bioquímicas de La Plata (INIBIOLP), CCT-La Plata, CONICET, Facultad de Ciencias Médicas
	Organization	Universidad Nacional de La Plata
	Address	La Plata, Argentina
	Email	smate@med.unlp.edu.ar

Abstract	The development of new strategies for achieving stable asymmetric membrane models has turned interleaflet lipid asymmetry into a topic of major interest. Cyclodextrin-mediated lipid exchange constitutes a simple and versatile method for preparing asymmetric membrane models without the need for sophisticated equipment. Here we describe a protocol for preparing asymmetric supported lipid bilayers mimicking membrane rafts by cyclodextrin-mediated lipid exchange and the main guidelines for obtaining structural information and quantitative measures of their mechanical properties using atomic force microscopy and force spectroscopy; two powerful techniques that allow membrane characterization at the nanoscale.

Keywords (separated by '-')	Membrane asymmetry - Lipid domains - Supported lipid bilayers - Lipid exchange - Cyclodextrins - Atomic force microscopy-force spectroscopy

Chapter 19

Formation and Nanoscale Characterization of Asymmetric Supported Lipid Bilayers Containing Raft-Like Domains

Romina F. Vázquez, Erasmo Ovalle-García, Armando Antillón, Iván Ortega-Blake, Carlos Muñoz-Garay, and Sabina M. Maté

Abstract

The development of new strategies for achieving stable asymmetric membrane models has turned interleaflet lipid asymmetry into a topic of major interest. Cyclodextrin-mediated lipid exchange constitutes a simple and versatile method for preparing asymmetric membrane models without the need for sophisticated equipment. Here we describe a protocol for preparing asymmetric supported lipid bilayers mimicking membrane rafts by cyclodextrin-mediated lipid exchange and the main guidelines for obtaining structural information and quantitative measures of their mechanical properties using atomic force microscopy and force spectroscopy; two powerful techniques that allow membrane characterization at the nanoscale.

Keywords Membrane asymmetry, Lipid domains, Supported lipid bilayers, Lipid exchange, Cyclodextrins, Atomic force microscopy-force spectroscopy

1 Introduction

During the last century, the use of lipid membrane model systems (e.g., free-standing bilayers, supported bilayers, monomolecular films at the air/water interface) has made a tremendous impact in the field of membrane biophysics allowing the study of structural and dynamical aspects of biomembranes. Asymmetric model systems are gaining increasing interest since they represent a more accurate version of biological membranes. Cells actively maintain an asymmetric distribution of phospholipids across the membrane with phosphatidylcholine and sphingolipid species mostly present in the outer leaflet; and phosphatidylserines, phosphatidylethanolamines, and phosphatidylinositols mainly located in the cytoplasmatic leaflet [1, 2]. In recent years, different methodologies for preparing asymmetric models have been developed and improved [3–9]. In particular, the exchange of outer membrane lipids

Charles G. Cranfield (ed.), *Membrane Lipids: Methods and Protocols*, Methods in Molecular Biology, vol. 2402,
https://doi.org/10.1007/978-1-0716-1843-1_19,

catalyzed by cyclodextrins (CDs) has been successfully applied to prepare asymmetric small, large, and giant unilamellar vesicles (SUVs, LUVs, GUVs) [7, 10, 11] and more recently, to produce asymmetric supported lipid bilayers (SLBs) [12, 13]. By taking advantage of the lipid solubilizing capacity of CDs [14], one specific lipid can be carried in soluble lipid-CDs complexes that interact with the external leaflet of the bilayer and deliver their cargo through lipid exchange, producing a local enrichment that generates asymmetry in the lipid composition. This approach has opened a new window to studies on the role of lipid asymmetry and its impact on membrane structure and function [15]. The architecture and properties of lipid domains, like the sphingolipids-enriched ordered domains (rafts) [16], in asymmetric systems are of particular interest to further the understanding of how lipid domains may form and act in vivo [17, 18].

Atomic force microscopy (AFM) is an outstanding technique to study the membrane organization at the nanoscale since it enables nanometer lateral resolution and angstrom vertical resolution in samples under physiological conditions and avoids the use of exogenous probes [19]. As a complement to AFM imaging, Force spectroscopy (FS) measurements can be performed to explore the nanomechanical properties of the bilayers which are related to lipid composition and phase behavior [20–23]. The combined AFM-FS techniques, therefore, provide nanometer/nanonewton resolution allowing the study of phase segregation and physical properties of the bilayers.

In this chapter, we describe a protocol for preparing asymmetric SLBs mimicking membrane rafts by CD-mediated lipid exchange suitable for AFM-FS measurements. Also given is a general overview on data acquisition and analysis to extract information about asymmetric membranes' structure and nanomechanics using those techniques. This experimental approach expands the applicability of membrane models allowing new studies on membrane properties and protein function in asymmetric environments.

2 Materials

2.1 Solutions

1. 2 mg/mL 1,2-Dioleoyl-*sn*-glycero-3-phosphocholine (DOPC) stock solution in HPLC grade chloroform or chloroform: methanol 2:1 (v/v).
2. 25 mg/mL *N*-palmitoyl-D-erythro-sphingosyl phosphorylcholine (SM) stock solution in HPLC grade chloroform or chloroform: methanol 2:1 (v/v) (*see* **Note 1**).
3. 1 mg/mL Cholesterol (Chol) stock solution in HPLC grade chloroform or chloroform:methanol 2:1 (v/v).

Store the lipid stock solutions in light safe glass vials hermetically closed at −20 °C (*see* **Note 2**).

4. HEPES-buffered saline (HBS Buffer), 20 mM HEPES, 150 mM NaCl, pH 7.4.
5. HBS-Ca^{2+} Buffer, 20 mM HEPES, 150 mM NaCl, 3 mM $CaCl_2$, pH 7.4.
6. Prepare the solutions in ultrapure Milli Q water (resistivity of 18.2 MΩ cm at 23 ± 1 °C), filter through 0.22 μm-pore-size filters, and keep them at 4 °C until use.
7. 30 mM Methyl-β-cyclodextrin solution in HBS Buffer (MβCD stock solution; *see* Subheading 3.1.2).

2.2 General Materials

1. Glass vials.
2. Glass microsyringes.
3. 1.5 mL light-proof microcentrifuge tubes.
4. Ultracentrifuge tubes.
5. 0.22 μm-pore-size filters.
6. Muscovite mica grade V-1.
7. Adhesive tape.
8. Silicon nitride cantilevers.

2.3 Equipment

1. Vacuum desiccator.
2. Bath sonicator.
3. Heating block.
4. Ultracentrifuge.
5. AFM microscope.

3 Methods

3.1 Preparation of MβCD-SM Complexes

3.1.1 Preparing SM Multilamellar Vesicles (MLVs)

1. Calculate the volume of the SM stock solution needed to prepare 333 μL of a 15 mM lipid suspension (*see* **Notes 3** and **4**).
2. Measure the calculated volume of the stock solution with a glass microsyringe and transfer it into a clean glass tube.
3. Evaporate the solvents under a stream of N_2 while gently rotating the tube to form a thin lipid film at the bottom of the tube.
4. Place the tube under vacuum overnight to further remove the solvents.
5. Add 333 μL of HBS Buffer prewarmed at 65 °C and let the lipids hydrate for 10 min at 65 °C (Fig. 1, Panel a).

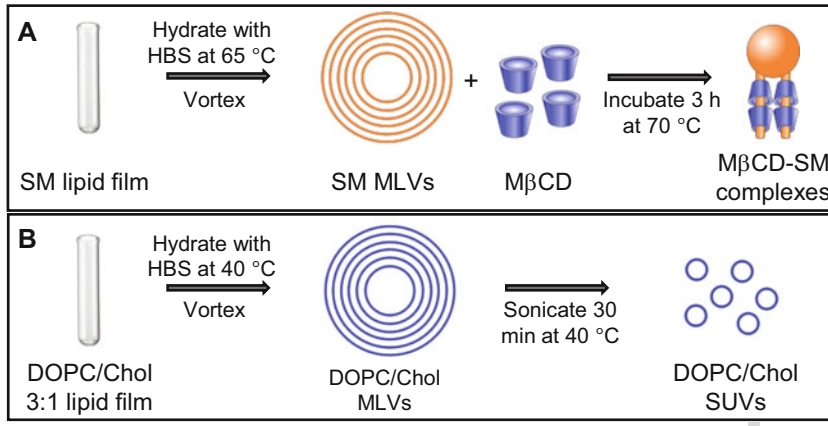

Fig. 1 Illustrated protocol for preparing MβCD-SM complexes and DOPC/Chol SUVs. Panel (**a**) schematic presentation of the SM MβCD solubilization process to assess soluble MβCD-SM complexes for lipid interchange. Panel (**b**) preparation of DOPC/Chol (3:1, mole ratio) SUVs for the subsequent formation of supported bilayers

6. Assist lipid dispersion by vigorous vortexing.
7. Reheat the lipid suspension to 65 °C for 10 min and repeat the vortex mix step. Repeat this procedure until complete lipid detachment (*see* **Note 5**).

3.1.2 Preparing MβCD Stock Solution

1. Calculate the amount of MβCD needed to prepare 667 μL of a 30 mM solution.
2. Weight the calculated mass in an analytical balance and dissolve MβCD in 667 μL of HBS Buffer at 65 °C.
3. Homogenize the solution using a vortex mixer.

3.1.3 Forming the MβCD-SM Complexes

1. Mix the 667 μL of the 30 mM MβCD solution with the 333 μL of 15 mM SM MLVs at 65 °C in a light-safe microcentrifuge tube (Fig. 1, Panel a). The final concentrations in the mixture will be 20 mM and 5 mM, respectively (*see* **Note 6**).
2. Incubate for 3 h at 70 °C in a dry heating block with continuous shaking (350 rpm) (*see* **Note 7**).
3. Divide the total volume according to the capacity of the available ultracentrifuge tubes (*see* **Note 8**).
4. Centrifuge at 54,000 × *g* for 20 min at 4 °C (*see* **Note 9**).
5. Carefully separate the supernatant containing the MβCD-SM complexes with a microsyringe.
6. Filter through 0.22 μm-pore-size syringe filters (*see* **Note 10**).
7. Aliquot the total volume and store the complexes at −20 °C until use.

3.2 DOPC/Chol (3:1 Mole Ratio) SUVs Preparation

1. Calculate the volumes of the DOPC and Chol stock solutions needed to prepare 500 μL (or the desired volume) of a 3:1 mole ratio 150 μM DOPC/Chol suspension (e.g., 22.10 μL of 2 mg/mL DOPC and 7.25 μL of 1 mg/mL Chol stock solutions for 500 μL).
2. Measure the appropriate volumes of the lipid solutions with a glass microsyringe and put them in a clean glass tube (*see* **Note 3**).
3. Mix the solution completely by vortexing.
4. Evaporate the solvents under a stream of N_2 gently rotating the tube during the procedure to form a thin lipid film at the bottom of the tube.
5. Place the tube under vacuum overnight to further remove the solvents (*see* **Note 11**).
6. Add 500 μL of HBS Buffer prewarmed at 40 °C to the tube and let the lipids hydrate for 5 min at 40 °C.
7. Vortex mix the hydrated lipids to form MLVs (Fig. 1, Panel b).
8. Put the lipids again at 40 °C for 5 min and repeat the vortex mix step. Repeat this procedure until complete lipid detachment.
9. Meanwhile, set the bath sonicator at 40 °C.
10. Introduce the tube in the bath sonicator at 40 °C and sonicate for 30 min to form SUVs (Fig. 1, Panel b) (*see* **Note 12**).

3.3 Formation of DOPC/Chol (3:1) SLBs

1. Attach the mica substrate to its corresponding support for AFM imaging according to the microscope set up.
2. Exfoliate the mica by peeling off the outer layer using adhesive tape. Repeat this until a uniform smooth mica layer is observed attached to the tape.
3. Add 100 μL of HBS-Ca^{2+} Buffer prewarmed at 40 °C to the surface of the mica and incubate 10 min at 40 °C.
4. Remove the Buffer.
5. Add 65 μL of the 150 μM DOPC/Chol 3:1 SUVs suspension at 40 °C to the surface of the mica.
6. Incubate for 20 min at 40 °C (Fig. 2) (*see* **Note 13**).
7. Gently remove the remaining suspension and wash 3 times with 60 μL of HBS Buffer at 40 °C (*see* **Note 14**).
8. Turn off the heating and let the sample cool and equilibrate at room temperature for 1.5 h.
9. Wash 10 times by adding 60 μL of HBS Buffer at room temperature each time to further remove the nonadsorbed vesicles, leaving 60 μL of fresh HBS Buffer on the surface of the mica after the last wash step.

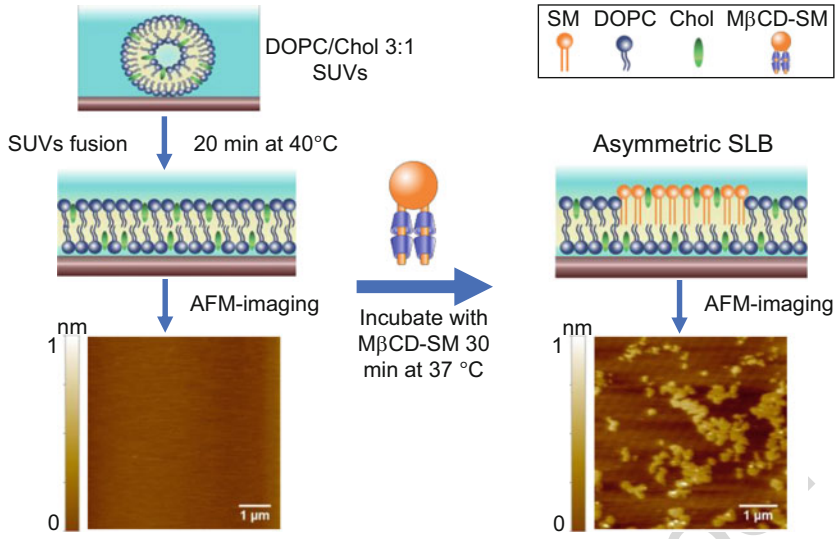

Fig. 2 Formation of asymmetric supported bilayers by lipid exchange. Schematic presentation of the vesicle fusion process to obtain DOPC/Chol (3:1 mole ratio) SLBs from SUVs (left schemes). The correct formation of DOPC/Chol (3:1) SLBs is confirmed by AFM imaging (lower left image). The DOPC/Chol bilayers are then incubated with MβCD-SM complexes to incorporate SM in the outer leaflet of the bilayers through lipid exchange, forming asymmetric SLBs (right scheme). After the incubation, the AFM images of asymmetric SLBs show lipid domains confirming the incorporation of SM (lower right image). (Adapted from Vázquez et al. 2021 [13], with permission from Elsevier)

10. Set the liquid cell of the AFM microscope at 24 °C, place the sample in the liquid cell, and let the sample equilibrate at 24 °C for at least 30 min.
11. Check the integrity of the SLB by AFM-imaging (Fig. 2) (*see* **Note 15**).

3.4 Formation of Asymmetric SLBs Through MβCD-Mediated Lipid Exchange

1. Set the liquid cell containing the DOPC/Chol SLB at 37 °C (*see* **Note 16**).
2. Prepare a fourfold dilution of the MβCD-SM stock solution in HBS Buffer (15 μL stock solution + 45 μL of HBS). This results in a solution with 5 mM nominal MβCD concentration (*see* **Note 17**).
3. Remove the HBS buffer on the surface of the DOPC/Chol SLB and add 60 μL of the MβCD-SM complex (Fig. 2).
4. Incubate at 37 °C for 30 min.
5. Remove the remaining suspension and delicately wash 15 times with 60 μL of HBS buffer at 37 °C. Leave 60 μL of fresh HBS buffer on the surface of the SLB and let the bilayer equilibrate at 24 °C.
6. Confirm SM incorporation and domain formation through AFM-imaging (Fig. 2).

3.5 AFM-Imaging and Force Spectroscopy Measurements

1. Mount the cantilevers in the atomic force microscope (*see* **Note 18**).
2. Calibrate the optical lever sensitivity for the cantilevers acquiring force curves in a lipid-free mica substrate and determine their spring constant using the thermal noise method [24] (*see* **Note 19**).
3. Place the liquid cell with the SLB in the AFM stage and let the system equilibrate at 24 °C for at least 30 min (*see* **Note 20**).
4. Set the microscope for contact mode and acquire large images (e.g., 20 μm × 20 μm) with 512 × 512-pixel resolution at a scanning rate of 1 Hz maintaining the minimum possible force. Collect images at different positions of the SLB to get a general picture of the membrane (*see* **Note 21**).
5. Acquire smaller images (10 μm × 10 μm or 5 μm × 5 μm) with 512 × 512-pixel resolution in regions where asymmetric lipid domains appear.
6. For measuring the height of the domains, flatten the images using a first-order plane correction and trace several line profiles through the image (Fig. 3) (*see* **Note 22**).
7. For force spectroscopic measurements, place a 16 × 16 grid (256 curves) over a representative area of the imaged bilayer (3 μm × 3 μm or 1 μm × 1 μm) and acquire force curves at 1 μm/s and 1 Hz with approach and retraction curves composed of 1024 (distance, force) ordered-pairs each (Fig. 3).
8. To process the collected data, plot the approach curves as force vs. tip-sample separation. Measure the breakthrough forces (Fb) and the rupture depths (d) at the region where a jump is detected in the curves that reflects a bilayer rupture event (Fig. 3). Calculate the Young's modulus (E) by fitting the indentation region of the curves using the classical Hertz contact model. Process the curves using a home-made software routine (*see* **Notes 23–25**).
9. Plot the histogram with the distributions from at least three independent sample preparations measured with at least three different tips (each sample prepared independently on a different day).
10. Obtain the Fb, d, and E values from Gaussian fittings of the data (*see* **Notes 26–28**).

4 Notes

1. Use saturated SM to prepare SLBs mimicking membrane rafts (with liquid-ordered (Lo)/liquid-disordered (Ld) phase coexistence) [22].

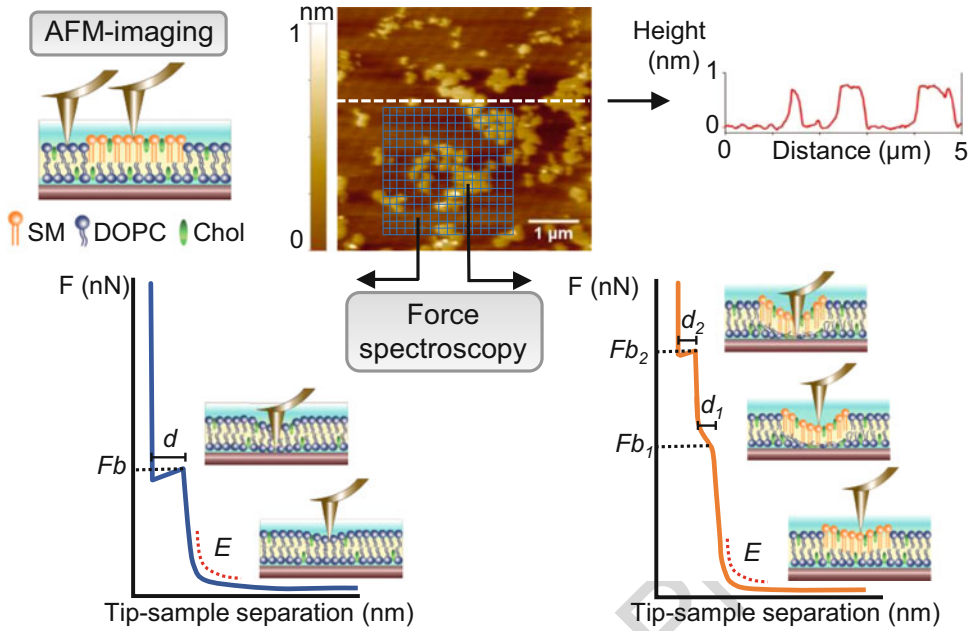

Fig. 3 Characterization of asymmetric SLBs through AFM microscopy and Force spectroscopy. A representative AFM image of an asymmetric SLB (DOPC/SM/Chol outer leaflet/DOPC/Chol inner leaflet) is presented in the figure. The height of the domains can be measured by tracing line profiles through the image, as shown for the dashed white line. After imaging, a 16 × 16 grid is placed over a representative area of the bilayer and force vs. distance curves acquired at each subregion of the grid (256 curves per grid) by Force spectroscopy. Force vs. distance curves are then transformed into Force vs. tip-sample separation curves like the ones shown in the figure. From these curves, the breakthrough force (Fb), and the rupture depths (*d*) can be measured at the region where a jump is detected that reflects a bilayer rupture event. The Young's modulus (*E*) can also be calculated by fitting the indentation region of the curves (red dotted lines) using the Hertz contact model. In this system, asymmetric Lo domains featured characteristic curves with two rupture events that could be attributed to an Ld phase that collapsed first at lower forces and then a Lo phase that ruptured secondly at higher Fb values (bottom right schemes). The continuous Ld phase showed single rupture events at low Fb values (bottom left schemes). (Adapted from Vázquez et al. 2021 [13], with permission from Elsevier)

2. Aliquot the dissolved lipids in brown vials, displace air with N_2 or other inert gas (Ar, He) previous to storage at −20 °C. Take care that the latter needs to be done every time the stock solutions are used. Due to solvent evaporation, the stock solutions become concentrated in time. Therefore, the lipid concentration should periodically be checked or the stock solutions divided into aliquots to be used in only a few experiments.
3. Using clean tubes and microsyringes throughout the whole procedure is critical for preparing lipid stocks and obtaining good quality samples for AFM imaging. Carefully wash the tubes and the glass syringes with chloroform:methanol 2:1 (v/v) before use to avoid contamination. For washing the tubes, include a small volume of this solvent, vigorously stir

in a vortex mixer, and then safely discard the solvent. Repeat this procedure at least 10 times. Microsyringes need to be carefully washed both before and after measuring each volume of lipid by filling the syringe and discarding the solvent, 10–15 times.

4. The volumes reported here yield 1 mL of MβCD-SM complexes. Lower volumes can be prepared according to the experimental needs and available ultracentrifuge tubes. MβCD-SM complexes can be stored at −20 °C for at least 3 months.
5. Usually, repeating this procedure 3 times is enough to achieve the complete detachment and resuspension of the lipid film, which can be evidenced by visual inspection of the bottom of the tube. This results in a milky suspension due to the high lipid concentration in the SM MLVs suspension.
6. Cyclodextrins are α-1,4-linked cyclic oligosaccharides that form truncated cone-shaped structures with a hydrophilic outside, that confers solubility in aqueous media, and a hydrophobic inner cavity which allows them to carry lipophilic guest molecules that fit in that cavity [25]. Specifically, MβCD molecules consist of seven glucopyranose units randomly methylated on the external hydroxyl groups (Fig. 4). MβCD has a high affinity for Chol molecules and is widely used at low concentrations to remove Chol from cell membranes. Notwithstanding, at high concentrations, MβCD can bind to phospholipids and solubilize phospholipid bilayers [14]. The cavity of MβCD has a diameter of ~0.6–0.65 nm and ~0.8 nm in height. Considering that a 16C acyl chain is ~2 nm in length, two MβCD molecules are proposed to bind to each acyl chain, therefore, forming MβCD-phospholipid complexes with 4:1 stoichiometry (Fig. 4). Results from calorimetric studies agree with this model [14].
7. The suspension should become clear after the incubation due to solubilization of MLVs.
8. Ultracentrifugation tubes should be filled to at least 2/3 of their maximum capacity to prevent collapsing of the walls.
9. Since most of the MLVs become solubilized, the pellet is sometimes difficult to detect. Mark the ultracentrifuge tubes previously to point out where the pellet is expected to appear. Set a free deceleration mode to prevent resuspension of the pellet.
10. Pre-wet the filter by passing HBS buffer through to reduce the dead volume.
11. Shorter times can be applied at this step by instead just keeping the lipids under vacuum for at least 2 h to assure complete solvent removal.

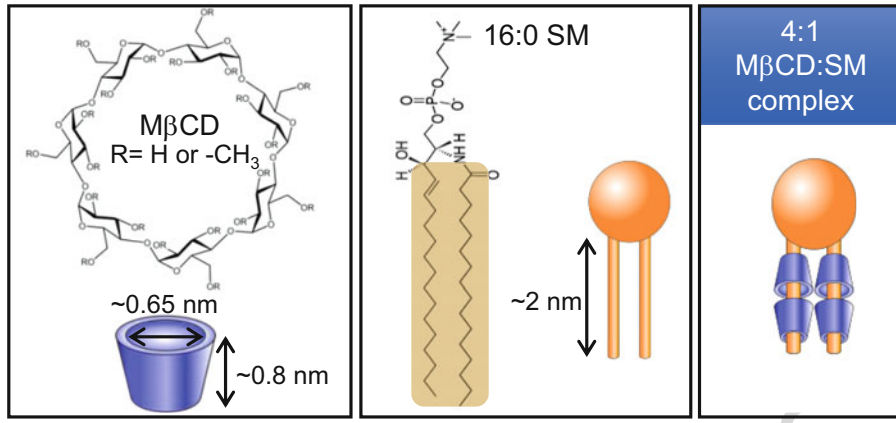

Fig. 4 MβCD-SM complex stoichiometry. Left Panel: chemical structure of MβCD, depicting the seven glucopyranose units and the sites of methylation (R). A scheme of the truncated cone-shaped structure of MβCD showing the diameter and height of its internal hydrophobic cavity is also presented. Middle Panel: chemical structure of palmitoyl-SM, the SM species used in these studies, with C16 chain lengths (highlighted in orange). The length of the hydrocarbon chains is depicted in the SM cartoon. Right panel: schematic representation of the 4:1 soluble complex formed between MβCD and SM used in the lipid exchange process

12. The 150 μM MLVs suspension is slightly cloudy and gets clear after sonication due to the formation of SUVs.
13. Monitor the amount of buffer on the surface of the SLB during the incubation and make sure that the sample does not get dry. Add small volumes (10–20 μL) of HBS buffer at 40 °C if needed.
14. Always leave a small amount of buffer on top of the SLB to maintain hydration of the lipid bilayer at all times. Be particularly gentle during the washing steps to avoid destroying the bilayer.
15. It is important to verify the formation of a defect-free DOPC/Chol bilayer that is completely covering the mica surface. This is to ensure the subsequent interaction of the MβCD-SM complexes with the SLB is only to the external leaflet of the bilayer.
16. In our experiments, the incorporation of SM at 37 °C led to the formation of Lo phases while performing the exchange at 24 °C resulted in a mixture of Lo and gel phases [13]. The incubation step can also be performed using a heating block separate from the stage of the AFM microscope.
17. Assuming that no MβCD is lost during the incubation with the SM MLVs or in the centrifugation step, the nominal MβCD concentration in the stock solution would be 20 mM. In our experiments, a 1/4 dilution of this stock solution of MβCD-SM complexes (resulting in a nominal 5 mM MβCD concentration) was appropriate for achieving asymmetric stable SLBs

with no major effects of MβCD on the overall Chol levels or bilayer integrity after the delivery of SM [13]. Higher MβCD-SM concentrations resulted in instability and damage of the SLBs.

18. In our studies, we used V-shaped cantilevers with nominal spring constants of 0.01–0.10 N/m and a 2 nm nominal tip radius [13]. Low spring constant cantilevers are suitable for AFM-imaging of lipid membranes as they exert low forces on the sample while sharp tips yield higher image resolution.
19. Many commercial AFMs contain built-in calibration *routines* based on the *thermal noise method* to perform this automatically. The calibration of the cantilevers is of most importance for accurately performing the subsequent force spectroscopy measurements.
20. To avoid thermal drift, it is important to equilibrate the SLBs with the microscope before imaging. In our experiments, this was accomplished in ~30 min, but longer times may be needed, depending on the conditions.
21. Once the tip is in contact with the surface, apply a sufficient force to ensure the tip maintains contact with the bilayer, but low enough to prevent deformation or damage of the SLB (typically <0.1 nN). Low scanning rates (<1 Hz) contribute to minimizing the friction forces.
22. Image processing and analysis can be performed using the AFM software or other commercially available software (e.g., Gwyddion free software). For statistical analysis, measure several domain heights in different images of at least three independent SLBs preparations.
23. Force vs. distance (*F*vs*D*) curves can be transformed to Force vs. Tip-sample Separation (*F*vs*S*) curves by calculating the Tip-sample separation (*S*) as:

$$S = D + \frac{F}{k_c} \tag{1}$$

where k_c is the calibrated cantilever spring constant. In this scheme, the signal of the rupture process is enhanced (Fig. 3). By taking the derivative of the Force, the highest peak yields the rupture force (Fb) while the width yields the penetration depth into the membrane (d). The bilayers Young's modulus (E) can be calculated by fitting the indentation region of *F*vs*S* curves using the classical Hertz contact model [26]:

$$F = \frac{4E\sqrt{R}\delta^{3/2}}{3(1-\nu^2)} \tag{2}$$

where F is the force, E the Young's modulus, R the tip radius, δ the indentation, and ν the Poisson ratio, taken as 0.5.

24. For more information on routines for data processing, please consult refs. 26 and 27.
25. In our experiments, the force curves acquired in asymmetric domains showed two rupture events that could be attributed to a Ld proximal hemilayer that collapsed first due to distal compression and a Lo outer hemilayer that was punctured by the tip in a second rupture event at higher applied forces (Fig. 3). The rupture depths (d) of each event agreed with these considerations. Symmetric Lo/Lo domains, instead, showed single rupture events [13].
26. Fb corresponds to the maximum force that the bilayer can withstand before rupture and represents an intrinsic property of the membrane related to the intermolecular interactions between the lipid molecules. Notice, though, that Fb values will vary with temperature, and buffer conditions (pH, ionic strength, presence of divalent cations) since those variables affect the mechanical stability of the bilayers [21, 28, 29]. Also, the chemical properties and geometry of the cantilever and the tip, the loading force, and approach velocity can all influence the Fb values measured [30–32].
27. The width of the breakthrough step (d) can be used as an estimation of the bilayer thickness at the rupture point. This depth represents a good estimation of the thickness of only the lipid bilayer, even when it is measured at a point in which the SLB is under compression, avoiding the contribution of the water molecules of the hydration layer [33].
28. E values reflect the resistance of the SLB against the elastic deformation induced by the tip in the indentation region. Notice that small variations in the tip's radius will affect the absolute values of the calculated Young's moduli. Also, consider that using small indenters, such as the 2 nm tips used in our studies, can yield lower Young's moduli than expected [32].

Acknowledgments

This work was supported by the Agencia Nacional de Promoción Científica y Tecnológica [PICT 881/2018], and the Consejo Nacional de Investigaciones Científicas y Técnicas (CONICET) [PIP 948/2017], Argentina, and Universidad Nacional Autónoma de México (UNAM) [DGAPA-PAPIIT-IG100920 and IN209318], and the Consejo Nacional de Ciencia y Tecnología (CONACyT) [PEI-252300], México. We thank Arturo Galván-Hernández from Laboratorio de Biofísica of the Instituto de Ciencias Físicas (ICF-UNAM) for technical assistance and Mario Raúl

Ramos from INIBIOLP for the graphic designs. R.F.V. and S.M.M. are members of the Carrera del Investigador of CONICET, Argentina.

References

1. Verkleij AJ, Zwaal RF, Roelofsen B, Comfurius P, Kastelijn D, van Deenen LL (1973) The asymmetric distribution of phospholipids in the human red cell membrane. A combined study using phospholipases and freeze-etch electron microscopy. Biochim Biophys Acta 323(2):178–193. https://doi.org/10.1016/0005-2736(73)90143-0
2. Daleke DL (2003) Regulation of transbilayer plasma membrane phospholipid asymmetry. J Lipid Res 44(2):233–242. https://doi.org/10.1194/jlr.R200019-JLR200
3. Takaoka R, Kurosaki H, Nakao H, Ikeda K, Nakano M (2018) Formation of asymmetric vesicles via phospholipase D-mediated transphosphatidylation. Biochim Biophys Acta Biomembr 1860(2):245–249. https://doi.org/10.1016/j.bbamem.2017.10.011
4. Hope MJ, Redelmeier TE, Wong KF, Rodrigueza W, Cullis PR (1989) Phospholipid asymmetry in large unilamellar vesicles induced by transmembrane pH gradients. Biochemistry 28(10):4181–4187. https://doi.org/10.1021/bi00436a009
5. Pautot S, Frisken BJ, Weitz DA (2003) Engineering asymmetric vesicles. Proc Natl Acad Sci U S A 100(19):10718–10721. https://doi.org/10.1073/pnas.1931005100
6. Hwang WL, Chen M, Cronin B, Holden MA, Bayley H (2008) Asymmetric droplet interface bilayers. J Am Chem Soc 130(18):5878–5879. https://doi.org/10.1021/ja802089s
7. Cheng HT, London ME (2009) Preparation and properties of asymmetric vesicles that mimic cell membranes: effect upon lipid raft formation and transmembrane helix orientation. J Biol Chem 284(10):6079–6092. https://doi.org/10.1074/jbc.M806077200
8. Lin Q, London E (2014) Preparation of artificial plasma membrane mimicking vesicles with lipid asymmetry. PLoS One 9(1):e87903. https://doi.org/10.1371/journal.pone.0087903
9. Hu PC, Li S, Malmstadt N (2011) Microfluidic fabrication of asymmetric giant lipid vesicles. ACS Appl Mater Interfaces 3(5):1434–1440. https://doi.org/10.1021/am101191d
10. Cheng HT, London E (2011) Preparation and properties of asymmetric large unilamellar vesicles: interleaflet coupling in asymmetric vesicles is dependent on temperature but not curvature. Biophys J 100(11):2671–2678. https://doi.org/10.1016/j.bpj.2011.04.048
11. Chiantia S, Schwille P, Klymchenko AS, London E (2011) Asymmetric GUVs prepared by MbetaCD-mediated lipid exchange: an FCS study. Biophys J 100(1):L1–L3. https://doi.org/10.1016/j.bpj.2010.11.051
12. Visco I, Chiantia S, Schwille P (2014) Asymmetric supported lipid bilayer formation via methyl-β-cyclodextrin mediated lipid exchange: influence of asymmetry on lipid dynamics and phase behavior. Langmuir 30(25):7475–7484. https://doi.org/10.1021/la500468r
13. Vázquez RF, Ovalle-García E, Antillón A, Ortega-Blake I, Bakás LS, Muñoz-Garay C, Maté SM (1863) Asymmetric bilayers mimicking membrane rafts prepared by lipid exchange: nanoscale characterization using AFM-Force spectroscopy. Biochim Biophys Acta Biomembr 2021(1):183467. https://doi.org/10.1016/j.bbamem.2020.183467
14. Anderson TG, Tan A, Ganz P, Seelig J (2004) Calorimetric measurement of phospholipid interaction with methyl-beta-cyclodextrin. Biochemistry 43(8):2251–2261. https://doi.org/10.1021/bi0358869
15. London E (2019) Membrane structure-function insights from asymmetric lipid vesicles. Acc Chem Res 52(8):2382–2391. https://doi.org/10.1021/acs.accounts.9b00300
16. Simons K, Ikonen E (1997) Functional rafts in cell membranes. Nature 387:569–572. https://doi.org/10.1038/42408
17. Lin Q, London E (2015) Ordered raft domains induced by outer leaflet sphingomyelin in cholesterol-rich asymmetric vesicles. Biophys J 108(9):2212–2222. https://doi.org/10.1016/j.bpj.2015.03.056
18. St Clair JW, Kakuda S, London E (2020) Induction of ordered lipid raft domain formation by loss of lipid asymmetry. Biophys J 119(3):483–492. https://doi.org/10.1016/j.bpj.2020.06.030
19. Alessandrini A, Facci P (2005) AFM: a versatile tool in biophysics. Meas Sci Technol 16(6):R65–R92. https://doi.org/10.1088/0957-0233/16/6/r01

20. Garcia-Manyes S, Sanz F (2010) Nanomechanics of lipid bilayers by force spectroscopy with AFM: a perspective. Biochim Biophys Acta 1798(4):741–749. https://doi.org/10.1016/j.bbamem.2009.12.019
21. Garcia-Manyes S, Redondo-Morata L, Oncins G, Sanz F (2010) Nanomechanics of lipid bilayers: heads or tails? J Am Chem Soc 132(37):12874–12886. https://doi.org/10.1021/ja1002185
22. Mate S, Busto JV, Garcia-Arribas AB, Sot J, Vazquez R, Herlax V, Wolf C, Bakas L, Goni FM (2014) N-nervonoylsphingomyelin (c24:1) prevents lateral heterogeneity in cholesterol-containing membranes. Biophys J 106(12):2606–2616. https://doi.org/10.1016/j.bpj.2014.04.054
23. Galvan-Hernandez A, Kobayashi N, Hernandez-Cobos J, Antillon A, Nakabayashi S, Ortega-Blake I (1862) Morphology and dynamics of domains in ergosterol or cholesterol containing membranes. Biochim Biophys Acta Biomembr 2020(2):183101. https://doi.org/10.1016/j.bbamem.2019.183101
24. Lévy R, Maaloum M (2001) Measuring the spring constant of atomic force microscope cantilevers: thermal fluctuations and other methods. Nanotechnology 13(1):33–37. https://doi.org/10.1088/0957-4484/13/1/307
25. Szejtli J (1998) Introduction and general overview of cyclodextrin chemistry. Chem Rev 98(5):1743–1754. https://doi.org/10.1021/cr970022c
26. Li JK, Sullan RM, Zou S (2011) Atomic force microscopy force mapping in the study of supported lipid bilayers. Langmuir 27(4):1308–1313. https://doi.org/10.1021/la103927a
27. Daza Millone MA, Vazquez RF, Mate SM, Vela ME (2018) Phase-segregated membrane model assessed by a combined SPR-AFM approach. Colloids Surf B: Biointerfaces 172:423–429. https://doi.org/10.1016/j.colsurfb.2018.08.066
28. Garcia-Manyes S, Oncins G, Sanz F (2005) Effect of temperature on the nanomechanics of lipid bilayers studied by force spectroscopy. Biophys J 89(6):4261–4274. https://doi.org/10.1529/biophysj.105.065581
29. Garcia-Manyes S, Oncins G, Sanz F (2005) Effect of ion-binding and chemical phospholipid structure on the nanomechanics of lipid bilayers studied by force spectroscopy. Biophys J 89(3):1812–1826. https://doi.org/10.1529/biophysj.105.064030
30. Richter RP, Brisson A (2003) Characterization of lipid bilayers and protein assemblies supported on rough surfaces by atomic force microscopy. Langmuir 19(5):1632–1640. https://doi.org/10.1021/la026427w
31. Sullan RM, Li JK, Hao C, Walker GC, Zou S (2010) Cholesterol-dependent nanomechanical stability of phase-segregated multicomponent lipid bilayers. Biophys J 99(2):507–516. https://doi.org/10.1016/j.bpj.2010.04.044
32. Saavedra VO, Fernandes TFD, Milhiet P-E, Costa L (2020) Compression, rupture, and puncture of model membranes at the molecular scale. Langmuir 36(21):5709–5716. https://doi.org/10.1021/acs.langmuir.0c00247
33. Attwood SJ, Choi Y, Leonenko Z (2013) Preparation of DOPC and DPPC supported planar lipid bilayers for atomic force microscopy and atomic force spectroscopy. Int J Mol Sci 14(2):3514–3539. https://doi.org/10.3390/ijms14023514